

Robust dynamic state estimation of power systems with model uncertainties based on adaptive unscented H_∞ filter

ISSN 1751-8687
 Received on 7th January 2019
 Revised 19th March 2019
 Accepted on 26th March 2019
 E-First on 16th May 2019
 doi: 10.1049/iet-gtd.2019.0031
 www.ietdl.org

Yi Wang^{1,2}, Yonghui Sun¹ ✉, Venkata Dinavahi², Kaike Wang³, Dongliang Nan^{3,4}

¹College of Energy and Electrical Engineering, Hohai University, Nanjing 210098, People's Republic of China

²Department of Electrical and Computer Engineering, University of Alberta, Edmonton, AB T6G 2V4, Canada

³Electric Power Research Institute State Grid Xinjiang Electric Power Co., Ltd, Urumqi 830010, People's Republic of China

⁴School of Electrical Engineering, Xinjiang University, Urumqi 830047, People's Republic of China

✉ E-mail: sunyonghui168@gmail.com

Abstract: This study considers the dynamic state estimation of power systems with model uncertainties that might be caused by the unknown noise statistics or unpredicted changes to the model parameters. To deal with these issues, an innovation-based estimator that is able to dynamically revise the statistics of system and measurement noise is proposed firstly. Then, based on the H_∞ criteria for bounding the adverse influences on the estimation error of model uncertainties and unscented transform technique, an adaptive strategy is developed to adjust the estimation error covariance matrix under various conditions. Finally, by incorporating the proposed approaches and H_∞ filter theory, a novel adaptive unscented H_∞ filter is established to realise dynamic state estimation of power system against model uncertainties. Extensive simulation results obtained from the IEEE-39 bus test system are presented to illustrate the effectiveness and robustness of the proposed method.

Nomenclature

δ	rotor angle
ω	rotor speed
e'_q	transient voltage along q axes
e'_d	transient voltage along d axes
T_m	mechanical torque
T_e	electric air-gap torque
H	inertia constant
K_D	damping factor
E_{fd}	internal field voltage
x_d	synchronous reactance at d axes
x_q	synchronous reactance at q axes
x'_d	transient reactance at d axes
x'_q	transient reactance at q axes
i_d	stator current at d axes
i_q	stator current at q axes

1 Introduction

1.1 Motivation

Reliable and accurate state estimation (SE) is of paramount importance for power system monitoring, protection, and control [1–4]. In general, SE methods of the power system can be grouped into two categories: static and dynamic SE. Static SE assumes that the power system operates under quasi-steady state, based on which the voltage phase angles and magnitude of all buses can be estimated by utilising the redundancy measurements from supervisory control and data acquisition or phasor measurement units (PMUs) [5]. Static SE plays an important role in the secure and reliable operation of power systems, which can provide the input data for some applications in the energy management system, such as optimal power flow and automatic generation control. However, it might not be competent for proper system monitoring and situational awareness due to the dynamics of the system are ignored. Therefore, accurate real-time dynamic states of the system acquired from the dynamic SE facilitated by the wide-area deployment of PMUs has become essential.

1.2 Literature review

To date, power system dynamic SE has been performed by various types of Kalman filters, such as the extended Kalman filter (EKF), unscented Kalman filter (UKF) and their variants [6–15]. In [6], based on the EKF, a lateral two-level dynamic SE method was proposed, which could deal with the increasing complexity and large data set successfully. In [7], the EKF with unknown inputs was developed for estimating the states and identifying the unknown inputs of power system simultaneously. In [8], by embedding the generalised maximum likelihood technique into the traditional EKF, a robust approach that exhibits robustness to observation and innovation outliers was acquired. In [9], a multi-step adaptive interpolation method was proposed to mitigate the adverse impact of non-linearity on the performance of EKF. However, the first-order Taylor series approximation-based EKF can only work well in a mild non-linear condition and easily lead to divergence. To circumvent these issues, several derivative-free filters were developed and applied to power system dynamic SE, such as the UKF approach [10–14], the particle filter [15], and the ensemble Kalman filter [16].

From the above literature review, it can be seen that Kalman-type filters play a vital role in power system dynamic SE. However, it should be noted that the aforementioned approaches work well only under conditions where the full knowledge of the power system dynamic SE model is available. To be specific, all parameters of the model and the noise statistics of process noise and measurement noise must be known accurately, which is practically infeasible, particularly for the real-time implementations [17–22]. Therefore, these methods are unable to deal with the cases of parameter uncertainties as well as unknown noise statistics of process and measurement. In practice, due to the unknown changes and disturbances of system inputs, the actual dynamic characteristics of a power system might not be predicted properly by the assumed dynamic model. Specifically, the measurement noise of PMUs may be unknown and does not follow a Gaussian distribution strictly [23, 24]. In addition, due to the aging process, magnetic saturation and changing temperature of the machine windings, the transient reactance of the generator and other parameters may be time-varying, leading to large model uncertainties [25]. These model uncertainties inevitably degrade

the performances of Kalman filter-based dynamic SE significantly, resulting in unreliable SE.

In recent years, in order to handle various uncertainties of the power system model, H_∞ filter has received considerable attention [18, 26–28]. Unlike the conventional Kalman filter that aims to achieve the minimum mean-square estimate, the H_∞ filter attempts to minimise the effect of the worst possible disturbances on the estimation error and consequently, it is more robust to model uncertainties. Motivated by this idea, the extended H_∞ filter was developed in [26, 27], but it inherits the weakness associated with EKF, which might not be suitable for the dynamic SE of power system with strong non-linearity. In addition, there are another two drawbacks in this method. First, the covariance matrices of system and measurement noise are still assumed constant during the process of dynamic SE, where their dynamic characteristics of changing with time are ignored. Secondly, in these methods, the finite upper bound of the model uncertainties need to be tuned artificially, which might be difficult for choosing the appropriate value in practical applications. Therefore, their practical application would be hampered.

1.3 Contributions and organisation

To address these issues, in this study, based on the H_∞ filter theory and unscented transform technique, a novel adaptive unscented H_∞ filter (AUHF) for power system dynamic SE against model uncertainties is proposed. The main contribution of this study is threefold.

- Based on the innovation information and the H_∞ criteria in robust control that bounds the influences of model uncertainties, an adaptive strategy is proposed to calculate the estimation error covariance matrix in a more appropriate way associated with the varying conditions. By using this strategy, not only the difficulty of choosing a suitable upper bound of estimation error is avoided, but also the adverse impacts of model uncertainties can be suppressed.
- An innovation-based estimator of noise statistics is also utilised to adjust the covariance matrices of system and measurement noise dynamically, which further enhances the robustness of AUHF to uncertain noise statistics.
- Extensive comparative experiments under different operating conditions have been implemented and it is confirmed that our proposed method can achieve a much better performance than the UKF [10], H_∞ extended Kalman filter (HEKF) [20] and unscented H_∞ filter (UHF) [28] methods for power system dynamic SE in the presence of model uncertainties.

The remainder of this paper is structured as follows. In Section 2, the dynamic SE model of the power system is established and analysed. In Section 3, the proposed AUHF approach is developed and introduced in detail. In Section 4, results of extensive simulations carried out on the IEEE-39 bus test system are provided to validate the efficacy of the developed method, and finally, conclusions are drawn in Section 5.

2 Dynamic SE model of power system

In this section, first, the continuous transient stability model of a synchronous generator is introduced. Then, by using a modified Euler method, the discrete state-space model for dynamic SE of the power system is acquired.

2.1 Continuous fourth-order transient model

In this study, the fourth-order transient stability model in a local d - q reference frame is utilised to estimate the states [15, 29, 30], which can be described by

$$\begin{cases} \dot{\delta} = \omega - \omega_0, \\ \dot{\omega} = \frac{\omega_0}{2H} \left(T_m - T_e - \frac{K_D}{\omega_0} (\omega - \omega_0) \right), \\ \dot{e}'_q = \frac{1}{T'_{d0}} (E_{fd} - e'_q - (x_d - x'_d) i_d), \\ \dot{e}'_d = \frac{1}{T'_{q0}} (-e'_d + (x_q - x'_q) i_q), \end{cases} \quad (1)$$

where δ represents the rotor angles in radian, ω is the rotor speeds in per unit, and $\omega_0 = 2\pi f_0$ indicates the synchronous speed; e'_q and e'_d represent the transient voltages along q and d axes; T_e and T_m denote the electric air-gap torque and the mechanical torque, respectively; H represents the inertia constant, and K_D denotes the damping factor; E_{fd} represents the internal field voltage; T'_{d0} and T'_{q0} denote the open circuit time constants in the d - q reference frame; x_d and x'_d are the synchronous reactance and the transient reactance at d axes, respectively; x_q and x'_q represent the synchronous reactance and the transient reactance along q axes, respectively; i_d and i_q denote the stator currents along local d and q axes.

To facilitate the notation, (1) can be further rewritten in a general state-space model as presented in (2) and (3)–(5)

$$\begin{cases} \dot{\mathbf{x}} = \mathbf{\Phi}_c(\mathbf{x}, \mathbf{u}) + \mathbf{w}_c, \\ \mathbf{y} = \mathbf{h}_c(\mathbf{x}, \mathbf{u}) + \mathbf{v}_c, \end{cases} \quad (2)$$

$$\mathbf{x} = [\delta \quad \omega \quad e'_q \quad e'_d]^T, \quad (3)$$

$$\mathbf{u} = [T_m \quad E_{fd} \quad i_R \quad i_I]^T, \quad (4)$$

$$\mathbf{y} = [\delta \quad \omega \quad e_R \quad e_I], \quad (5)$$

where \mathbf{x} represents the state vector, \mathbf{u} denotes the known input vector; \mathbf{y} is the output vector, note that the rotor angle δ and rotor speed ω can be directly measured by utilising the algorithms in PMUs [31, 32]; $\mathbf{\Phi}_c(\cdot)$ and $\mathbf{h}_c(\cdot)$ represent the state transition function and output function, respectively. The subscript c denotes the continuous time model; \mathbf{w}_c and \mathbf{v}_c are the process and output noise, respectively; e_R and i_R represent the stator voltage and current at the R axes, respectively; e_I and i_I denote the stator voltage and current at the I axes, respectively.

In order to transform (1) into the general state-space model in (2) and acquire the state transition function $\mathbf{\Phi}_c(\cdot)$, i_d , i_q are written as functions of x and u

$$i_d = i_R \sin(\delta) - i_I \cos(\delta), \quad (6)$$

$$i_q = i_I \sin(\delta) + i_R \cos(\delta). \quad (7)$$

Similarly, to obtain the output function $\mathbf{h}_c(\cdot)$, e_R and e_I are written as functions of x and u

$$e_R = (e'_d + i_q x'_q) \sin(\delta) + (e'_q - i_d x'_d) \cos(\delta), \quad (8)$$

$$e_I = (e'_q - i_d x'_d) \sin(\delta) - (e'_d + i_q x'_q) \cos(\delta). \quad (9)$$

2.2 Discrete state-space model

To realise the dynamic SE utilising the discrete measurements, the continuous time model in (2) needs to be further discretised into its discrete form as

$$\begin{cases} \mathbf{x}_k = \mathbf{\Phi}(\mathbf{x}_{k-1}, \mathbf{u}_{k-1}) + \mathbf{w}_k, \\ \mathbf{y}_k = \mathbf{h}(\mathbf{x}_k, \mathbf{u}_k) + \mathbf{v}_k, \end{cases} \quad (10)$$

where k represents the time instant at $k\Delta t$, Δt indicates the sampling interval, \mathbf{w}_k and \mathbf{v}_k denote the process and measurement

noise vectors that are supposed to be Gaussian with zero-mean, follow the covariance matrices $\hat{\xi}_k$ and \hat{R}_k , respectively. The discrete state transition function $\Phi(\cdot)$ can be acquired by utilising the modified Euler approach [33] as

$$\tilde{\mathbf{x}}_k = \mathbf{x}_{k-1} + \Phi_c(\mathbf{x}_{k-1}, \mathbf{u}_{k-1})\Delta t, \quad (11)$$

$$\tilde{\mathbf{f}} = \frac{\Phi_c(\tilde{\mathbf{x}}_k, \mathbf{u}_k) + \Phi_c(\mathbf{x}_{k-1}, \mathbf{u}_{k-1})}{2}, \quad (12)$$

$$\mathbf{x}_k = \mathbf{x}_{k-1} + \tilde{\mathbf{f}}\Delta t. \quad (13)$$

Also, the output function \mathbf{h}_c can be directly discretised by

$$\mathbf{y}_k = \mathbf{h}_c(\mathbf{x}_k, \mathbf{u}_k) + \mathbf{v}_k. \quad (14)$$

The discrete state-space model in (10) can be utilised to implement power system dynamic SE based on various methods.

3 Proposed AUHF

In this section, based on the H_∞ filter theory and the unscented transform technique, by incorporating the proposed innovation-based estimator of noise statistics and the estimation covariance matrix adaptive update approach, a novel AUHF against various model uncertainties is designed.

3.1 Derivation of the AUHF

According to the H_∞ filter theory in [18], a robust filter that effectively bounds the adverse influences of the model uncertainties can be acquired by satisfying the following criteria:

$$\sup_{\{\mathbf{x}_0, \mathbf{v}_k, \mathbf{w}_k\}} \frac{\sum_{k=0}^{N_t-1} \|\mathbf{x}_k - \hat{\mathbf{x}}_k\|_{\hat{P}_{k-1}}^2}{\|\mathbf{x}_0 - \hat{\mathbf{x}}_0\|_{\hat{P}_0}^2 + \left(\sum_{k=0}^{N_t-1} \|\mathbf{w}_k\|_{\hat{\xi}_k}^2 + \|\mathbf{v}_k\|_{\hat{R}_k}^2\right)} < \gamma, \quad (15)$$

where γ is a given positive scalar parameter that bounds the model uncertainties; N_t indicates the maximum iteration time; \mathbf{x}_k and $\hat{\mathbf{x}}_k$ are the true state vector and its estimation results, respectively; \mathbf{x}_0 and \hat{P}_0 represent the initial state vector and its covariance matrix, respectively; \hat{P}_k is the estimated covariance matrix; $\hat{\xi}_k$ and \hat{R}_k are the respective covariance matrices of process noise and measurement noise at time instant k , which could be estimated by the proposed approach in the next part of this Section.

In order to obtain a more accurate and reliable dynamic SE result of the power system with model uncertainties, in this part, a robust dynamic state estimator is developed. The proposed AUHF method consists of three main steps: state prediction, state filtering, and adaptive update of the estimation error covariance utilising the criteria in (15).

Step 1: state prediction: By assuming the SE $\hat{\mathbf{x}}_{k-1} \in \mathbb{R}^{n \times 1}$ and the associated estimation error covariance $\hat{P}_{x,k-1} \in \mathbb{R}^{n \times n}$ have been acquired at time instant $k-1$, the state prediction can proceed as follows:

- i. *Sigma point generation:* Based on the unscented transformation technique [34], by utilising the SE information at time instant $k-1$, $2n+1$ sigma points can be generated through

$$\chi_k^l = \hat{\mathbf{x}}_{k-1}, l = 0, \quad (16)$$

$$\chi_k^l = \hat{\mathbf{x}}_{k-1} \pm \left(\sqrt{(n+\kappa)\hat{P}_{x,k-1}}\right)_l, \quad l = 1, 2, \dots, 2n, \quad (17)$$

where n represents the dimension of state variables, κ indicates the scaling parameter defined as $\kappa = \alpha^2(n+k_f) - n$, and α is a constant usually chosen from $[10^{-4}, 1]$; k_f is a constant, which

is usually set as 0 for dynamic SE; $\sqrt{(\cdot)}$ denotes the operation of Cholesky decomposition.

- ii. *State prediction:* The sigma points are propagated through the state transition function, then the predicted state vector $\tilde{\mathbf{x}}_k$ and the associated prediction error covariance matrix $\tilde{P}_{x,k}$ can be calculated by

$$\tilde{\chi}_k^j = \Phi(\chi_k^j), \quad (18)$$

$$\tilde{\mathbf{x}}_k = \sum_{j=0}^{2n} W_j \tilde{\chi}_k^j, \quad (19)$$

$$\tilde{P}_{x,k} = \sum_{j=0}^{2n} W_j (\tilde{\chi}_k^j - \tilde{\mathbf{x}}_k)(\tilde{\chi}_k^j - \tilde{\mathbf{x}}_k)^T + \hat{\xi}_k, \quad (20)$$

where $j = 0, 1, 2, \dots, 2n$, W_j are the weights defined as

$$W_0 = \frac{\kappa}{n+\kappa}, \quad W_j = \frac{\kappa}{2(n+\kappa)}, \quad j = 1, 2, \dots, 2n. \quad (21)$$

- iii. *Measurement prediction:* The sigma points are instantiated through the output function, and then the predicted measurement $\tilde{\mathbf{y}}_k$ and its covariance $\tilde{P}_{y,k}$ can be derived as

$$\tilde{\eta}_k^j = \mathbf{h}(\tilde{\chi}_k^j), \quad (22)$$

$$\tilde{\mathbf{y}}_k = \sum_{j=0}^{2n} W_j \tilde{\eta}_k^j, \quad (23)$$

$$\tilde{P}_{y,k} = \sum_{j=0}^{2n} W_j (\tilde{\eta}_k^j - \tilde{\mathbf{y}}_k)(\tilde{\eta}_k^j - \tilde{\mathbf{y}}_k)^T + \hat{R}_k. \quad (24)$$

- iv. *Cross-correlation covariance calculation:* Calculate the cross-covariance matrix $P_{xy,k}$ between the predicted states and the predicted measurements

$$P_{xy,k} = \sum_{j=0}^{2n} W_j (\tilde{\chi}_k^j - \tilde{\mathbf{x}}_k)(\tilde{\eta}_k^j - \tilde{\mathbf{y}}_k)^T. \quad (25)$$

Step 2: state filtering: Based on the predicted state, the filtered state $\hat{\mathbf{x}}_k$ can be achieved by utilising the available measurements \mathbf{y}_k at time instant k

$$\mathbf{K}_k = P_{xy,k} \tilde{P}_{y,k}^{-1}, \quad (26)$$

$$\hat{\mathbf{x}}_k = \tilde{\mathbf{x}}_k + \mathbf{K}_k(\mathbf{y}_k - \tilde{\mathbf{y}}_k), \quad (27)$$

where \mathbf{K}_k denotes the Kalman gain at time instant k , $(\cdot)^{-1}$ represents the inversion of a matrix.

Step 3: estimation error covariance update: By utilising the statistical linear error propagation approach in [35], the measurement covariance matrix $\tilde{P}_{y,k}$ and the cross-correlation covariance $P_{xy,k}$ can be approximated by

$$\tilde{P}_{y,k} \approx \mathbf{H}_k \tilde{P}_{x,k} \mathbf{H}_k^T + \hat{R}_k, \quad (28)$$

$$P_{xy,k} \approx \tilde{P}_{x,k} \mathbf{H}_k^T, \quad (29)$$

where $\mathbf{H}_k = (\partial \mathbf{h}(\mathbf{x}_k) / (\partial \mathbf{x}_k))|_{\mathbf{x}_k = \tilde{\mathbf{x}}_k}$ represents the Jacobin matrix of output function at time instant k .

Based on the extended H_∞ filter in [20,26], by utilising formulas (28) and (29), the estimation error covariance $\hat{P}_{x,k}$ that satisfies criteria (15) can be derived as follows:

$$\hat{P}_{x,k} = \tilde{P}_{x,k} - [P_{xy,k} \tilde{P}_{y,k}^{-1} \mathbf{R}_k^{-1}] \begin{bmatrix} P_{xy,k}^T \\ \tilde{P}_{x,k}^T \end{bmatrix} \quad (30)$$

and

$$\mathbf{R}_{e,k} = \begin{bmatrix} \tilde{\mathbf{P}}_{y,k} & \mathbf{P}_{xy,k}^T \\ \mathbf{P}_{xy,k} & -\gamma^2 \mathbf{L}_k \mathbf{L}_k^T + \tilde{\mathbf{P}}_{x,k} \end{bmatrix}, \quad (31)$$

where $\mathbf{L}_k \in \mathbb{R}^{n \times n}$ represents a diagonal matrix to be designed and the tuning parameter γ can be obtained by searching over $\gamma > 0$ such that $\tilde{\mathbf{P}}_{x,k} > 0$.

Applying the matrix inversion lemma to (30) yields

$$\hat{\mathbf{P}}_{x,k}^{-1} = \tilde{\mathbf{P}}_{x,k}^{-1} + \tilde{\mathbf{P}}_{x,k}^{-1} \mathbf{P}_{xy,k} \tilde{\mathbf{R}}_k^{-1} \left[\tilde{\mathbf{P}}_{x,k}^{-1} \mathbf{P}_{xy,k} \right]^T - \gamma^{-2} (\mathbf{L}_k \mathbf{L}_k^T)^{-1}. \quad (32)$$

Therefore, in order to avoid the difficulty in choosing an appropriate value for γ in [20, 26] and achieving a better SE performance, here, matrix \mathbf{L}_k is designed as

$$\mathbf{L}_k = \left(\gamma \sqrt{\tilde{\mathbf{P}}_{x,k}^{-1} + \tilde{\mathbf{P}}_{x,k}^{-1} \mathbf{P}_{xy,k} \tilde{\mathbf{R}}_k^{-1} \left[\tilde{\mathbf{P}}_{x,k}^{-1} \mathbf{P}_{xy,k} \right]^T - \varphi_{\max}^{-2} \mathbf{I}} \right)^{-1}, \quad (33)$$

where $\sqrt{(\cdot)}$ denotes the Cholesky decomposition, $\varphi_{\max}^2 \mathbf{I}$ indicates the upper bound of the $\hat{\mathbf{P}}_k$, which is obtained by the physical information of the practical systems.

Nevertheless, it should be noted that the use of the upper bound $\varphi_{\max}^2 \mathbf{I}$ might be too conservative, where too much emphasis is placed on accommodating the worst condition (largest model uncertainties) at the expense of optimality. In order to improve the robustness of the developed method without decreasing accuracy, an adaptive strategy to adjust $\hat{\mathbf{P}}_k$ in response to the dynamically changing environment is given as follows:

$$\hat{\mathbf{P}}_{x,k} = \begin{cases} \tilde{\mathbf{P}}_{x,k} - \mathbf{K}_k \tilde{\mathbf{P}}_{y,k} \mathbf{K}_k^T & \text{if } \tilde{\mathbf{P}}_{y,k} > \alpha \tilde{\mathbf{P}}_{v,k}, \\ \tilde{\mathbf{P}}_{x,k} - [\mathbf{P}_{xy,k} \tilde{\mathbf{P}}_{x,k}] \mathbf{R}_{e,k}^{-1} \begin{bmatrix} \mathbf{P}_{xy,k}^T \\ \tilde{\mathbf{P}}_{x,k}^T \end{bmatrix} & \text{otherwise,} \end{cases} \quad (34)$$

where $\tilde{\mathbf{P}}_{v,k} = \mathbf{E}(\nu_k \nu_k^T | \tilde{\mathbf{x}}_{k-1})$ denotes the real covariance matrix of the innovation $\nu_k = \mathbf{y}_k - \tilde{\mathbf{y}}_k$ at time instant k , $\alpha > 0$ is a scalar parameter that provides an extra degree of freedom to tune the threshold during the implementation. Though $\tilde{\mathbf{P}}_{v,k}$ is unknown in practice, it can be estimated by

$$\tilde{\mathbf{P}}_{v,k} = \begin{cases} \nu_k \nu_k^T, & \text{if } k = 0, \\ \frac{\rho \tilde{\mathbf{P}}_{v,k-1} + \nu_k \nu_k^T}{\rho + 1}, & \text{else } k > 0, \end{cases} \quad (35)$$

where ρ represents a forgetting factor and usually set as $\rho = 0.98$ [36].

Remark 1: It is worth pointing out that the bound of $\hat{\mathbf{x}}_k$ can be controlled by enlarging the estimation error covariance matrix $\hat{\mathbf{P}}_k$ [37]. Therefore, in the design of an extended H_∞ filter [20, 26], by setting the \mathbf{L}_k as an identity matrix \mathbf{I} , $\hat{\mathbf{P}}_k$ could be enlarged by decreasing λ to acquire stronger robustness, but it is difficult to choose a suitable λ to guarantee $\hat{\mathbf{P}}_k$ is sufficiently large. This problem can be solved by designing \mathbf{L}_k as (27), where not only the difficulty in tuning the parameter λ is avoided, but also the requirements of $\hat{\mathbf{P}}_k$ can be satisfied.

Remark 2: With the specific design in (34), when the innovation is large, the estimation error covariance matrix $\hat{\mathbf{P}}_k$ will be set as $\tilde{\mathbf{P}}_{x,k} - [\mathbf{P}_{xy,k} \tilde{\mathbf{P}}_{x,k}] \mathbf{R}_{e,k}^{-1} [\mathbf{P}_{xy,k} \tilde{\mathbf{P}}_{x,k}]^T$, which can mitigate the adverse effects of model uncertainties and avoid the proposed method divergence; on the contrary, while the innovation is rather small, $\hat{\mathbf{P}}_k$

will be set as $\tilde{\mathbf{P}}_{x,k} - \mathbf{K}_k \tilde{\mathbf{P}}_{y,k} \mathbf{K}_k^T$, so that the SE results will not be distorted.

3.2 Estimation of noise covariance matrices

For a practical power system, its system model is inevitable with uncertainties and the statistics of measurement noise may change from time to time, yielding unknown and time varying $\boldsymbol{\xi}$ and \mathbf{R} [22]. Therefore, in order to accommodate the changeable noise environment of the power system and further enhance the robustness of the proposed method, the covariance matrices of process noise and measurement noise should be revised dynamically.

Based on the work in [38], by utilising the innovation information, a modified Sage–Husa noise estimator is introduced to dynamically revise the covariance matrices of process noise and measurement noise, which can be implemented by

$$\hat{\boldsymbol{\xi}}_k = (1 - d_{k-1}) \hat{\boldsymbol{\xi}}_{k-1} + d_{k-1} (\mathbf{K}_k \nu_k \nu_k^T \mathbf{K}_k^T + \hat{\mathbf{P}}_k), \quad (36)$$

$$\hat{\mathbf{R}}_k = \hat{\mathbf{R}}_{k-1} \cdot \text{diag}(\exp^{-\nu_{kl}}), \quad (37)$$

where $d_{k-1} = (1 - b)/(1 - b^k)$ and $b \in [0.95, 0.995]$ is a constant parameter; $\hat{\boldsymbol{\xi}}_k$ denotes the estimation covariance matrix of process noise, $\hat{\mathbf{R}}_k$ represents the estimation covariance matrix of measurement noise at time instant k , \exp is the exponential function with the natural constant e as the base.

Remark 3: By using the proposed noise statistic estimator, the covariance matrices of process noise and measurement noise can be adjusted dynamically with the actual operating conditions of the power system, which further enhances the robustness and stability of the proposed method, and a much better estimation performance can be achieved.

For convenience, the proposed AUHF approach for robust dynamic SE of power systems with model uncertainties is fully summarised as Algorithm 1 (see Fig. 1).

4 Numerical results

4.1 Test system and simulation studies

In this section, extensive simulations are conducted on the New England test system model with ten machines and 39 buses to demonstrate the performance of the designed approach against various sources of uncertainties. The single-line diagram of this test system is shown in Fig. 2 and its detailed parameters can be found in [39]. To mimic the responses of a real power system, the transient stability simulations are implemented to generate measurements and true state variables utilising the software PSCAD/EMTDC. In addition, in order to capture the dynamics and reduce integration errors, the trapezoidal integration method is adopted with a time step of 1/120 s to solve the differential and algebraic equations. The simulations consist of the following steps: a three-phase fault is applied to bus 16 at $t = 0.5$ s to simulate a system disturbance, where the fault impedance is 0.001 pu and the fault is cleared at $t = 0.7$ s; the rotor angle, rotor speed and the stator voltages along R and I axes of the generator are corrupted by additive noise to simulate the realistic PMU measurements, noted that the sampling rate for the measurements in all case studies is 50 frames per second [40–42]. The parameters α and forgetting factor ρ are set to 10^{-3} and 0.98, respectively. For the state initialisation, the steady-state values are utilised. Due to the space limitation, only the estimated results of generator 9 are presented for illustration purposes.

Generally, while using the filtering-based methods to estimate the dynamic states of the power system, the statistics of system and measurement noise are usually assumed to be known exactly in advance. However, for a practical power system, the real noise statistics are usually difficult to acquire accurately [20]. In addition, the process and measurement noise might change over

- 1: Initialization: Set initial values for $\hat{x}_0, \hat{P}_0, \hat{\xi}_0, \hat{R}_0, \alpha, N_t$;
- 2: Input: T_m, E_{fd}, i_R, i_I and measurement y_k ;
- 3: **while** $k = 0$ to N_t **do**
- 4: **step 1:** calculate the prediction state and error covariance matrix according to the Eqs. (17)-(21)
- 5:
$$\tilde{x}_k \leftarrow \sum_{j=0}^{2n} W_j \tilde{X}_k^j;$$
- 6:
$$\tilde{P}_k \leftarrow \sum_{j=0}^{2n} W_j (\tilde{X}_k^j - \tilde{x}_k) (\tilde{X}_k^j - \tilde{x}_k)^T + \hat{\xi}_k;$$
- 7: **step 2:** obtain the cross-correlation covariance matrix according to the Eqs. (22)-(25)
- 8:
$$P_{xy,k} \leftarrow \sum_{j=0}^{2n} W_j (\tilde{X}_k^j - \tilde{x}_k) (\eta_k^j - \tilde{y}_k)^T;$$
- 9: **step 3:** compute the estimation state by the Eqs. (26) and (27)
- 10:
$$\hat{x}_k \leftarrow \tilde{x}_k + K_k (y_k - \tilde{y}_k);$$
- 11: **step 4:** adaptive update the estimation error covariance matrix according to the Eqs. (28)-(35)
- 12: **if** $\hat{P}_{y,k} > \alpha \hat{P}_{\nu,k}$ **then**
- 13:
$$\hat{P}_{x,k} \leftarrow \tilde{P}_{x,k} - K_k \tilde{P}_{y,k} K_k^T;$$
- 14: **else**
- 15:
$$\hat{P}_{x,k} \leftarrow \tilde{P}_{x,k} - [P_{xy,k} \tilde{P}_{x,k}] R_{e,k}^{-1} \begin{bmatrix} P_{xy,k}^T \\ \tilde{P}_{x,k}^T \end{bmatrix};$$
- 16: **end if**
- 17: **step 5:** estimate the covariance matrices of process noise and measurement noise
- 18:
$$\hat{\xi}_k \leftarrow (1 - d_{k-1}) \hat{\xi}_{k-1} + d_{k-1} (K_k \nu_k \nu_k^T K_k^T + \hat{P}_k);$$
- 19:
$$\hat{R}_k \leftarrow \hat{R}_{k-1} \cdot \text{diag}(\exp^{-|\nu_k|});$$
- 20: **step 6:** output $\hat{x}_k, \hat{P}_{x,k}$ and time update
- 21: $k \leftarrow k + 1;$
- 22: **end while**

Fig. 1 Algorithm 1: AUHF

time, yielding unknown non-Gaussian statistics [23]. On the other hand, due to the aging process and variations of generator operating temperature, some constant parameters that are not changed by default may change with time [25]. Last but not least, for a real-time application, the computational efficiency is another paramount factor. Due to the estimation of the current time step need to be completed before the measurements of the next time instant arrive, therefore, in order to comprehensively assess the performance of the AUHF method against model uncertainties and the computational efficiency, based on the test system, the following four comparative experiments are carried out:

Case study 1: The UKF [10], HEKF [20], UHF [28] and proposed AUHF approach are considered and compared for the test system with unknown Gaussian process and measurement noises.

Case study 2: The discussed methods are implemented for the test system with the unknown non-Gaussian process and measurement noises.

Case study 3: The robustness of UKF, HEKF, UHF, and AUHF to uncertain parameters of the state-space model is analysed and compared.

Case study 4: The computational efficiency of the four discussed approaches under case studies 1–3 is investigated and compared.

In addition, in order to acquire more general and significant simulation results, $N_{MC} = 200$ Monte–Carlo simulations are run for case studies 1–3. The notions of mean absolute error (MAE) and average SE error index E_x are adopted to evaluate the estimation accuracy and average estimation performance of the discussed approaches, which are defined as follows:

$$\text{MAE}(k) = \frac{1}{N_{MC}} \sum_{j=1}^{N_{MC}} \frac{1}{N_s} \sum_{i=1}^{N_s} |x_{i,k}^{\text{est}} - x_{i,k}^{\text{true}}|, \quad (38)$$

$$E_x = \frac{1}{N_{MC}} \sum_{j=1}^{N_{MC}} \sqrt{\sum_{k=1}^{N_t} (x_{i,k}^{\text{est}} - x_{i,k}^{\text{true}})^2 / N_t}, \quad (39)$$

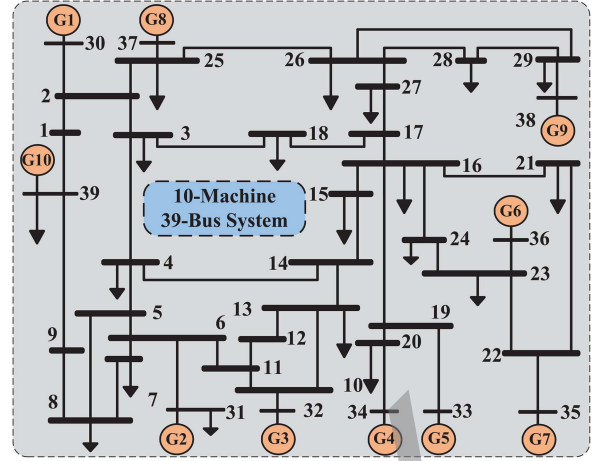


Fig. 2 Single-line diagram of 10-machine 39-bus test system

where N_s is the number of states; $x_{i,k}$ denotes the types of states that can be δ, ω, e'_q or e'_d at time instant k ; $x_{i,k}^{\text{est}}$ indicates the estimated state; $x_{i,k}^{\text{true}}$ indicates the associated true value; N_t represents the number of total time steps.

4.2 Case study 1: unknown Gaussian process and measurement noises

Generally, in the dynamic SE of the power system, the noise statistics of process and measurement are usually assumed to be normally distributed with zero means, their covariance matrices are $\xi = 10^{-6} I_{4 \times 4}$ and $R = 10^{-6} I_{4 \times 4}$, respectively. However, for practical power systems, the process noise and measurement noise may be varied under the different operating conditions, yielding deviations from nominal values. In such a scenario, the accurate information of the noise statistics cannot be acquired. Thus, in this case study, the noise statistics of process noise and measurement are assumed unknown. The initial covariance matrices of process noise and measurement noise are set as $\xi = 10^{-5} I_{4 \times 4}$ and $R = 10^{-4} I_{4 \times 4}$, respectively.

In order to evaluate the performance of UKF, HEKF, UHF and the proposed AUHF methods to this type of uncertainty, all of them are utilised to estimate the dynamic states of generator 9 (G9). Fig. 3 shows the estimated results of the components of the process and measurement noise covariance matrices (due to the page limitation, only the estimated results of q_1 and r_1 are presented, where q_1, r_1 indicate the first element of system and measurement noise covariance matrices, respectively). It can be observed that the proposed innovation-based noise statistical estimator can revise the covariance matrices timely, which is important for effectively binding their adverse effects. The SE results of each discussed method are displayed in Figs. 4 and 5. Fig. 6 further presents the MAE results of each algorithm were calculated from 200 Monte–Carlo simulations. The comparison of average estimation error E_x results that were calculated from 200 Monte–Carlo simulations are presented in Table 1. As can be seen from these SE results, the performance of UKF is heavily affected by the mismatched covariance matrices. The UHF and HEKF approaches outperform UKF, as they can bind the estimation errors to some extent. However, as UHF and HEKF cannot revise the mismatched initial covariance matrices dynamically and adaptively update the estimation covariance matrix responding under varying conditions; thus their estimation errors are still large. In contrast, with the utilisation of the dynamic correction technique, the proposed AUHF achieves the best performance of the discussed methods, which exhibits strong robustness to the noise uncertainties.

4.3 Case study 2: unknown non-Gaussian process and measurement noises

For a practical power system, the measurement noise associated with PMUs may deviate from the Gaussian assumption, which has

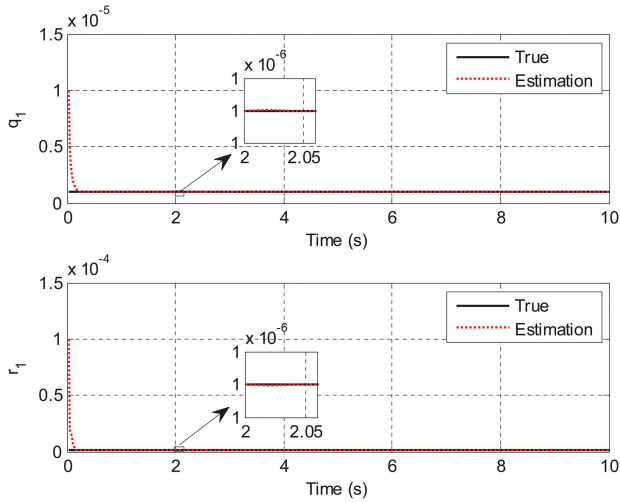


Fig. 3 Estimated results of the component of system noise covariance matrix q_1 and the component of measurement noise covariance matrix r_1 for case study 1

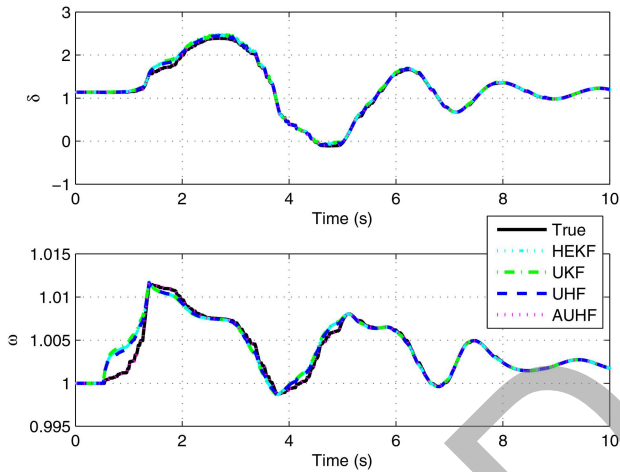


Fig. 4 Estimated results of δ , ω for G9 with unknown Gaussian process and measurement noises

been demonstrated in [23, 43]. Therefore, in order to investigate the robustness of each discussed method to the unknown non-Gaussian process and measurement noises, the covariance matrices of process noise and measurement noise are assumed to follow a Gaussian mixture model with two mixture components, where the 2% data of the covariance matrices are contaminated by $\xi = 10^{-5}I_{4 \times 4}$ and $R = 10^{-5}I_{4 \times 4}$ while the remaining 98% data are set as the true covariance matrices $\xi = 10^{-6}I_{4 \times 4}$ and $R = 10^{-6}I_{4 \times 4}$.

The simulation results of this case are shown in Figs. 7–10. To be specific, the estimated results of the components of process and measurement noise covariance matrices are displayed in Fig. 7. It is observed from this figure that the noise covariance matrices can be tracked accurately. Figs. 8 and 9 display the comparison results of the four discussed approaches in terms of estimating the states of G9. In addition, the MAE results of each algorithm that were calculated from 200 Monte–Carlo simulations is shown in Fig. 10. Table 2 further provides the average estimation error E_x of each method that was calculated from 200 Monte–Carlo simulations. As can be seen from these test results, the performance of UKF is degraded significantly, especially for the poor estimates of transient voltage e'_d . In contrast, the HEKF and UHF can achieve a slightly better estimation result than UKF, due to their bounding the uncertainties to a certain degree. However, due to HEKF and UHF not being able to track the variations of noise covariance matrices and the estimation error covariance matrix not being updated corresponding to the different conditions, their estimation accuracy is much lower than the proposed AUHF approach.

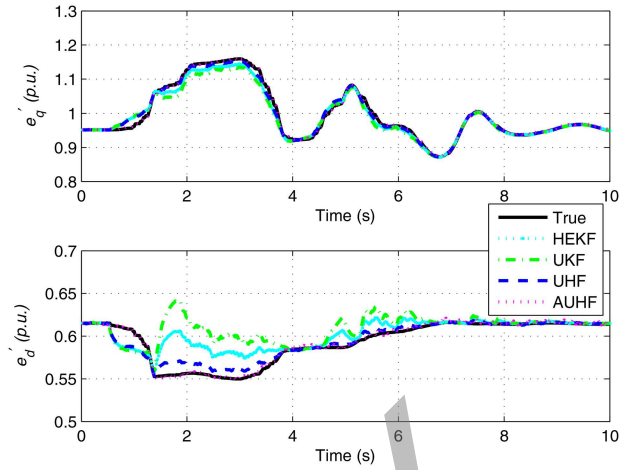


Fig. 5 Estimated results of e'_q , e'_d for G9 with unknown Gaussian process and measurement noises

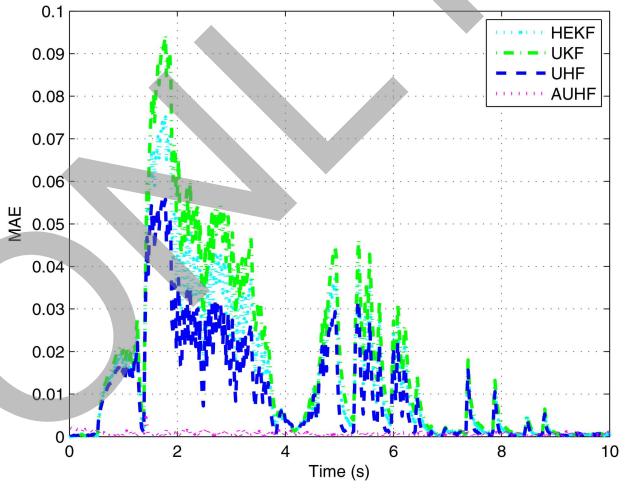


Fig. 6 MAE results of each algorithm for G9 with unknown Gaussian process and measurement noises

Table 1 Average estimation error E_x of G9 for case study 1

Methods	δ	ω	e'_q	e'_d
UKF	0.0468	0.0151	0.0168	0.0278
HEKF	0.0410	0.0108	0.0118	0.0172
UHF	0.0313	0.0069	0.0079	0.0073
AUHF	0.0015	0.0018	0.0021	0.0020

To further demonstrate the performance of the proposed method against non-Gaussian noises, the following scenario is considered: where the covariance matrices of process noise are assumed to follow a Gaussian mixture model with two mixture components, where the 5% data of the covariance matrices are contaminated by $\xi = 10^{-5}I_{4 \times 4}$ while the remaining 95% data are set as the true covariance matrices $\xi = 10^{-6}I_{4 \times 4}$; a Laplace noise with zero mean and scale 0.01 is added to the measurements. The average estimation error E_x of the discussed approaches that were calculated from 200 Monte–Carlo simulations is shown in Table 3. It can be observed from these test results that due to the increased degree of process noises deviate from nominal values and the effects of Laplace measurement noises, the performance of UKF degraded seriously and the average estimation error of it is very large. HEKF and UHF can achieve slightly higher estimation accuracy than UKF, which shows that the HEKF and UHF can mitigate the adverse effects of non-Gaussian noises to some extent. However, their incremental average estimation errors are still significant. In contrast, the proposed AUHF method is still able to effectively bind the estimation error caused by non-Gaussian noise, yielding much better estimation results than the other approaches.

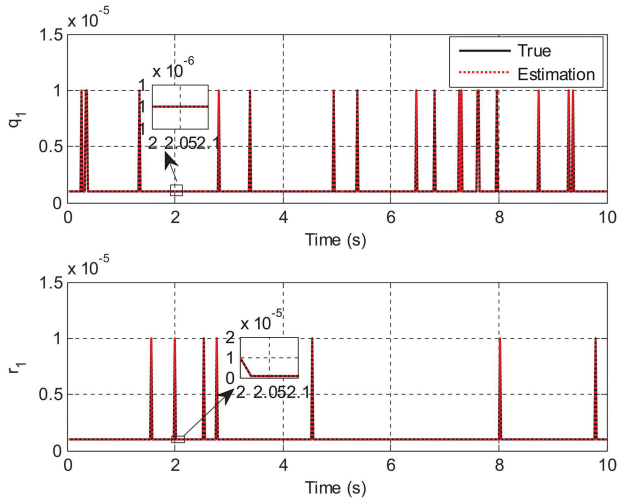


Fig. 7 Estimated results of the component of system noise covariance matrix q_1 and the component of measurement noise covariance matrix r_1 for case study 2

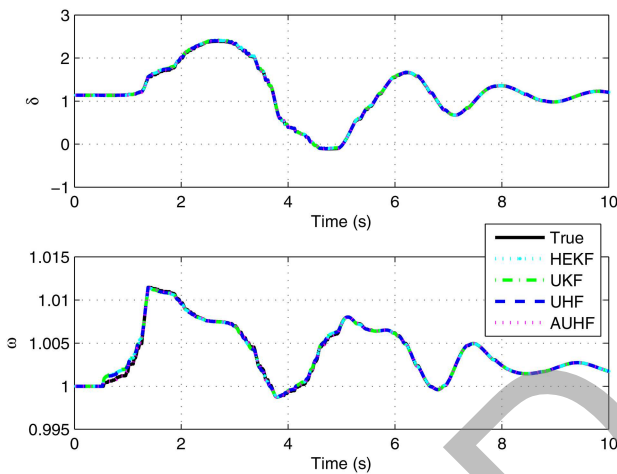


Fig. 8 Estimated results of δ , ω for G9 with the unknown non-Gaussian process and measurement noises

These comparisons further verify the superior performance of the proposed method against unknown non-Gaussian noises.

4.4 Case study 3: uncertain parameters of the state-space model

Due to the aging processes, the changing machine temperature during its operation and other reasons, some parameters that are not changed by default may change over time, such as the reactance and transient reactance [13]. Therefore, in order to assess the robustness of the proposed AUHF method against the uncertain parameters of state-space model, in this scenario, it is assumed that there is 20% error in the d -axis and q -axis transient reactance, which can be simulated by a Gaussian random variable with zero mean and given error as standard deviation.

The simulation results of this scenario are displayed in Figs. 11–13. To be specific, Fig. 11 shows the estimated results of δ and ω for G9. Fig. 12 displays the estimated results of the associated states e'_q and e'_d . The MAE results of each discussed method that were calculated from 200 Monte–Carlo simulations are shown in Fig. 13. In addition, the average estimation error E_x of each discussed approach was calculated from the 200 Monte–Carlo simulations provided in Table 4. As is expected, due to UKF lack of robustness, it cannot bind the uncertainties. Therefore, its performance is degraded seriously, which has the largest average SE error of all the discussed approaches. On the other hand, the HEKF and UHF can mitigate the adverse impacts caused by the uncertain parameters of the state-space model to a certain degree,

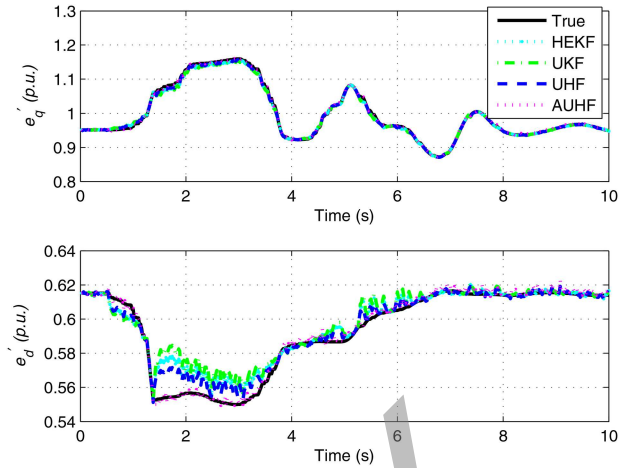


Fig. 9 Estimated results of e'_q , e'_d for G9 with the unknown non-Gaussian process and measurement noises

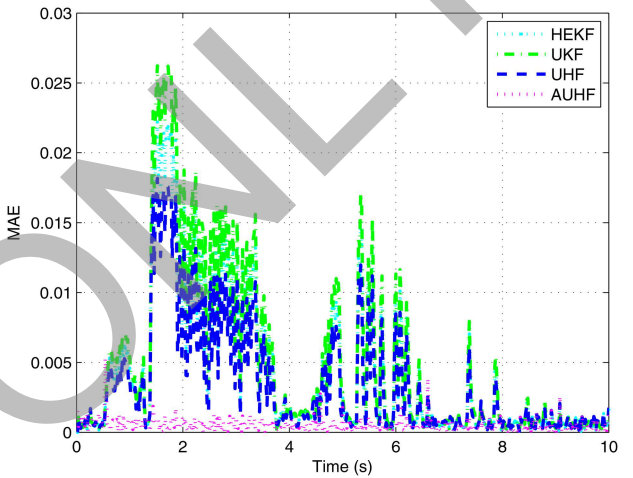


Fig. 10 MAE results of each algorithm for G9 with the unknown non-Gaussian process and measurement noises

Table 2 Average estimation error E_x of G9 for case study 2

Methods	δ	ω	e'_q	e'_d
UKF	0.0117	0.0064	0.0054	0.0090
HEKF	0.0102	0.0067	0.0045	0.0072
UHF	0.0086	0.0048	0.0036	0.0052
AUHF	0.0010	0.0027	0.0023	0.0022

Table 3 Average estimation error E_x of G9 for case study 2

Methods	δ	ω	e'_q	e'_d
UKF	0.1929	0.0249	0.0164	0.0892
HEKF	0.0317	0.0203	0.0140	0.0237
UHF	0.0237	0.0173	0.0107	0.0223
AUHF	0.0016	0.0015	0.0014	0.0028

but their accuracy of SE is much lower than the proposed AUHF method. In contrast, the AUHF method can effectively bound the adverse effects of uncertainties and present reasonably good SE results. For example, as can be seen in Fig. 12, it can be found that the estimation errors of e'_q and e'_d by utilising the UKF, HEKF and UHF approaches are increased significantly. However, the estimation errors of the proposed AUHF are still much smaller than the other three approaches. This is due to the fact that the proposed AUHF method can adaptively update the estimation covariance matrix to respond to the changing parameters. These comparison results confirm the superior performance of the proposed AUHF method against uncertain parameters of the state-space model.

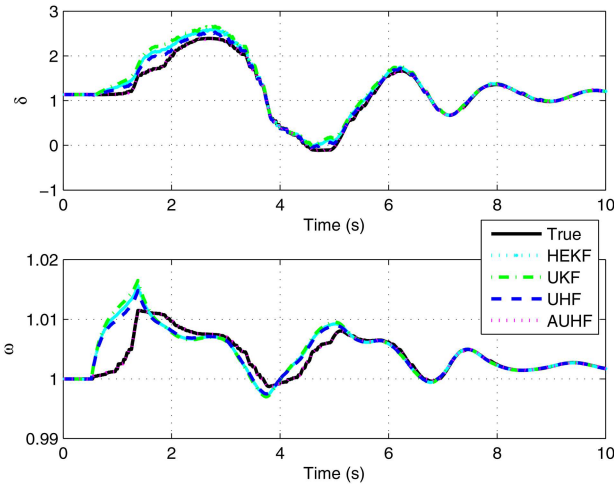


Fig. 11 Estimated results of δ , ω for G9 with uncertain parameters of the state-space model

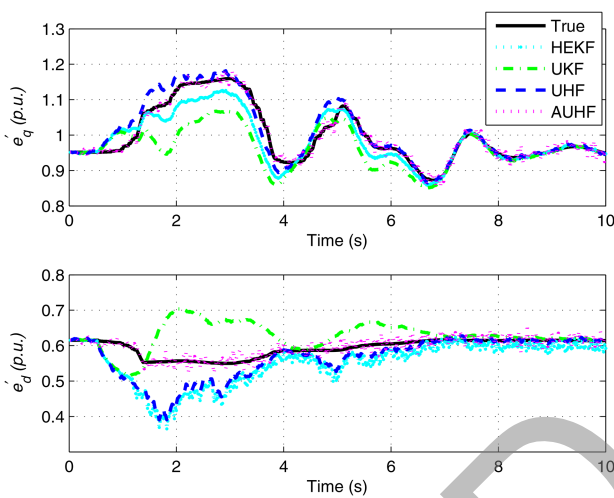


Fig. 12 Estimated results of e'_q , e'_d for G9 with uncertain parameters of the state-space model

4.5 Case study 4: assessment of computational efficiency

For a real-time application, computing time is another paramount factor of an algorithm. To estimate the states of power systems in real time, estimation of the current time step needs to be completed before the measurements of the next time instant arrive. In other words, a dynamic SE approach must be enough fast to keep up with the measurements data flow. Therefore, in order to validate the applicability of the proposed AUHF approach for online estimation with a PMU sampling rate of 50 samples per second, the execution time of each discussed approach in the case studies 1–3 is investigated and compared. It has to be mentioned that all the tests are implemented in the MATLAB environment using a computer with Intel Core CPU i5-6500 @ 3.2 GHz and 8-GB RAM.

The total computational time of all the discussed methods under different cases is displayed in Fig. 14. It is worth pointing out that the time reported here is implemented in Matlab and is not fully optimised, which can be more efficient by C-based code and further optimisation. From these comparisons, it can be observed that the total execution time of AUHF is the largest under each case study, followed by the HEKF, UHF, and UKF, which is expected since it needs to dynamically revise the noise covariance matrices and adaptively update the estimation covariance matrix. Furthermore, the reason why the HEKF costs slightly more times is that it involves the Jacobian computation. In addition, the UHF method spends a little bit time than UKF, due to more equations. More importantly, although the execution time of the AUHF is a little bit longer, it is still much smaller than the PMU sampling

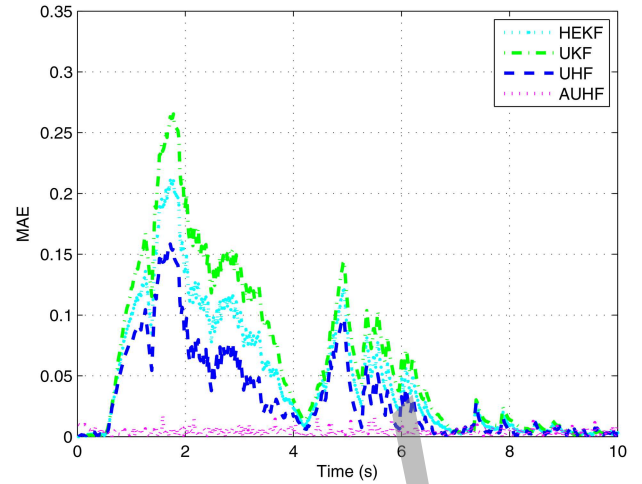


Fig. 13 MAE results of each algorithm for G9 with uncertain parameters of the state-space model

Table 4 Average estimation error E_x of G9 for case study 3

Methods	δ	ω	e'_q	e'_d
UKF	0.1658	0.0369	0.0579	0.0623
HEKF	0.1226	0.0241	0.0312	0.0567
UHF	0.0828	0.0189	0.0253	0.0486
AUHF	0.0097	0.0032	0.0117	0.0134

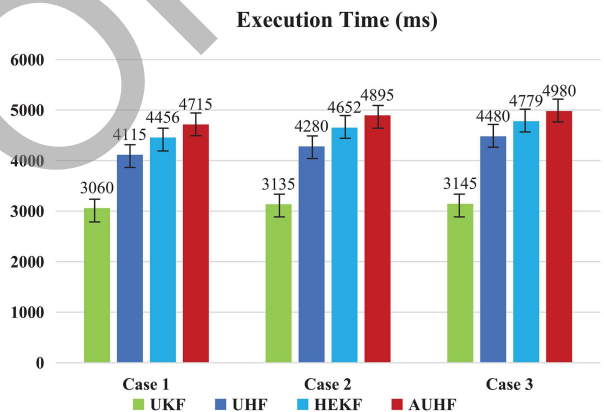


Fig. 14 Total execution time of each method in the case studies 1–3

period (20 ms for 50 samples/s), which demonstrates that it can be implemented in real-time.

5 Conclusions

This study proposed an AUHF for power system dynamic SE against various sources of uncertainties. It has the following excellent features:

- the use of the innovation-based noise statistic estimator is able to dynamically revise the covariance matrices of process noise and measurement noise, which plays an important role in bounding the adverse effects of the noise statistical uncertainties;
- by utilising the H_∞ criteria and unscented transform technique, an innovation-based adaptive strategy was designed to dynamically update the estimation error covariance matrix. As a result, the estimation error caused by various uncertainties can be bounded, and higher accuracy of SE can be achieved.
- extensive comparison results carried out on the IEEE 39-bus test system under various operating conditions confirmed that the proposed approach has much better robustness than other alternatives, which is more suitable for practical implementation.

In addition, due to the excellent scalability of the proposed AUHF method, it is convenient and meaningful to expand it to a more generalised AUHF approach, which is left for our future work.

6 Acknowledgments

This work was supported in part by the National Natural Science Foundation of China under grant no. 61673161, in part by the Natural Science Foundation of Jiangsu Province of China under grant no. BK20161510, in part by the Fundamental Research Funds for the Central Universities of China under grant no. 2017B655X14, in part by Six Talent Peaks High Level Project of Jiangsu Province under grant no. XNY-004, in part by the Postgraduate Research & Practice Innovation Program of Jiangsu Province under grant no. KYCX17_0484, and in part by the Natural Science and Engineering Research Council (NSERC) of Canada. The work of Yi Wang was supported by the China Scholarship Council.

7 References

- [1] Jiang, T., Bai, L., Li, F., *et al.*: 'Synchrophasor measurement-based correlation approach for dominant mode identification in bulk power systems', *IET Gener. Transm. Distrib.*, 2016, **10**, (11), pp. 2710–2719
- [2] Geetha, S.J., Saikat, C., Ketan, R.: 'Hierarchical parallel dynamic estimator of states for interconnected power system', *IET Gener. Transm. Distrib.*, 2018, **12**, (10), pp. 2299–2306
- [3] Sharma, A., Suresh, C.S., Saikat, C.: 'Multi-agent-based dynamic state estimator for multi-area power system', *IET Gener. Transm. Distrib.*, 2016, **10**, (1), pp. 131–141
- [4] Jiang, T., Jia, H., Zhao, J., *et al.*: 'Mode matching pursuit for estimating dominant modes in bulk power grid', *IET Gener. Transm. Distrib.*, 2014, **8**, (10), pp. 1677–1686
- [5] Qi, J.J., Sun, K., Wang, J.H., *et al.*: 'Dynamic state estimation for multi-machine power system by unscented Kalman filter with enhanced numerical stability', *IEEE Trans. Smart Grid*, 2018, **9**, (2), pp. 1184–1196
- [6] Karimipour, H., Dinavahi, V.: 'Extended Kalman filter-based parallel dynamic state estimation', *IEEE Trans. Smart Grid*, 2015, **6**, (3), pp. 1539–1549
- [7] Ghahremani, E., Kamwa, L.: 'Dynamic state estimation in power system by applying the extended Kalman filter with unknown inputs to phasor measurements', *IEEE Trans. Power Syst.*, 2011, **26**, (4), pp. 2556–2566
- [8] Zhao, J.B., Netto, M., Mili, L.: 'A robust iterated extended Kalman filter for power system dynamic state estimation', *IEEE Trans. Power Syst.*, 2017, **32**, (4), pp. 3205–3216
- [9] Akhlaghi, S., Zhou, N., Huang, Z.: 'A multi-step adaptive interpolation approach to mitigating the impact of nonlinearity on dynamic state estimation', *IEEE Trans. Smart Grid*, 2018, **9**, (4), pp. 3102–3111
- [10] Valverde, G., Terzija, V.: 'Unscented Kalman filter for power system dynamic state estimation', *IET Gener. Transm. Distrib.*, 2011, **5**, (1), pp. 29–37
- [11] Risso, M., Rubiales, A.J., Lotito, P.A.: 'Hybrid method for power system state estimation', *IET Gener. Transm. Distrib.*, 2014, **9**, (7), pp. 636–643
- [12] Karimipour, H., Dinavahi, V.: 'Parallel relaxation-based joint dynamic state estimation of large-scale power systems', *IET Gener. Transm. Distrib.*, 2016, **10**, (2), pp. 452–459
- [13] Anagnostou, G., Pal, B.C.: 'Derivative-free Kalman filtering based approaches to dynamic state estimation for power systems with unknown inputs', *IEEE Trans. Power Syst.*, 2018, **33**, (1), pp. 116–130
- [14] Zhao, J.B.: 'Power system dynamic state estimation considering measurement correlations', *IEEE Trans. Energy Convers.*, 2017, **32**, (4), pp. 1630–1632
- [15] Zhou, N., Meng, D., Lu, S.: 'Estimation of the dynamic states of synchronous machines using an extended particle filter', *IEEE Trans. Power Syst.*, 2013, **28**, (4), pp. 4152–4161
- [16] Zhou, N., Meng, D., Huang, Z., *et al.*: 'Dynamic state estimation of a synchronous machine using PMU data: A comparative study', *IEEE Trans. Smart Grid*, 2018, **6**, (1), pp. 450–460
- [17] Grewal, M.S., Andrews, A.P.: '*Kalman filtering*' (Wiley Press, New York, NY, USA, 2008)
- [18] Simon, D.: '*Optimal state estimation*' (Wiley Press, New York, NY, USA, 2006)
- [19] Li, H.Y., Zhang, Z.X., Xie, X.P.: 'Adaptive event-triggered fuzzy control for uncertain active suspension systems', *IEEE Trans. Cybern.*, 2018, DOI: 10.1109/TCYB.2018.2864776 to appear
- [20] Zhao, J.B.: 'Dynamic state estimation with model uncertainties using H_{∞} extended Kalman filter', *IEEE Trans. Power Syst.*, 2018, **33**, (1), pp. 1099–1100
- [21] Zhao, J.B., Mili, L.: 'Robust unscented Kalman filter for power system dynamic state estimation with unknown noise statistics', *IEEE Trans. Smart Grid*, 2017, **10**, (2), pp. 1215–1224, DOI: 10.1109/TSG.2017.2761452
- [22] Wang, Y., Sun, Y.H., Wei, Z.N., *et al.*: 'Parameters estimation of electromechanical oscillation with incomplete measurement information', *IEEE Trans. Power Syst.*, 2018, **33**, (5), pp. 5016–5028
- [23] Wang, S., Zhao, J.B., Huang, Z., *et al.*: 'Assessing Gaussian assumption of PMU measurement error using field data', *IEEE Trans. Power Del.*, 2018, **33**, (6), pp. 3233–3236
- [24] Huang, Z.Y., Zhou, N., Diao, R.S., *et al.*: 'Capturing real-time power system dynamics: opportunities and challenges'. Proc. IEEE Power Engineering Society General Meeting, Denver, CO, USA, July 2018, pp. 1–5
- [25] Zhao, J.B., Mili, L.: 'A decentralized H-infinity unscented Kalman filter for dynamic state estimation against uncertainties', *IEEE Trans. Smart Grid*, 2018, DOI: 10.1109/TSG.2018.2870327 to appear
- [26] Einicke, G.A., White, L.B.: 'Robust extended Kalman filtering', *IEEE Trans. Signal Process.*, 1999, **47**, (9), pp. 2596–2599
- [27] Seo, J., Yu, M., Park, C.G., *et al.*: 'An extended robust H_{∞} filter for nonlinear constrained uncertain systems', *IEEE Trans. Signal Process.*, 2006, **54**, (11), pp. 4471–4475
- [28] Li, W.L., Jia, Y.M.: 'H-infinity filtering for a class of nonlinear discrete-time systems based on unscented transform', *Signal Process.*, 2010, **90**, (12), pp. 3301–3307
- [29] Huang, Z., Du, P., Kosterev, D., *et al.*: 'Generator dynamic model validation and parameter calibration using phasor measurements at the point of connection', *IEEE Trans. Power Syst.*, 2013, **28**, (2), pp. 1939–1949
- [30] Sauer, P.W., Pai, M.A.: '*Power system dynamics and stability*' (Prentice-Hall Press, Upper Saddle River, NJ, USA, 1998)
- [31] Xie, X.R., Xiao, J.Y., Li, J., *et al.*: 'A new approach to estimate power angle of synchronous generators'. Proc. of the CSEE, 2003, **23**, (11), pp. 106–110
- [32] Jha, M., Chakrabarti, S., Kyriakides, E.: 'Estimation of the rotor angle of a synchronous generator by using PMU measurements'. Proc. IEEE Eindhoven PowerTech, Eindhoven, Netherlands, July 2015, pp. 1–6
- [33] Kundur, P.: '*Power system stability and control*' (McGraw-Hill Press, New York, NY, USA, 1994)
- [34] Uhlmann, J.K.: 'Simultaneous map building and localization for real time applications'. PhD thesis, University of Oxford, 1994
- [35] Sibley, G., Suckhatme, G., Matthies, L.: 'The iterated Sigma point Kalman filter with application to long range stereo', *Robot.: Sci. Syst.*, 2006, **8**, (1), pp. 235–244
- [36] Bai, M., Zhou, D., Schwarz, H.: 'Identification of generalized friction for an experimental planar two-link flexible manipulator using strong tracking filter', *IEEE Trans. Robot. Autom.*, 1999, **15**, (2), pp. 362–369
- [37] Xiong, K., Zhang, H., Liu, L.: 'Adaptive robust extended Kalman filter for nonlinear stochastic systems', *IET Control Theory Appl.*, 2008, **2**, (3), pp. 239–250
- [38] Zhao, L., Wang, X., Sun, M., *et al.*: 'Adaptive UKF filtering algorithm based on maximum a posteriori estimation and exponential weighting', *Acta Autom. Sin.*, 2011, **36**, (7), pp. 1007–1019
- [39] Canizares, C., Fernandes, T., Geraldi, J., *et al.*: 'Benchmark systems for small-signal stability analysis and control'. *IEEE PES Task Force, Technical Report*, 2015
- [40] Martin, K.E., Benmouyal, G., Adamiak, M.G., *et al.*: 'IEEE standard for synchrophasor measurements for power systems', *IEEE Trans. Power Del.*, 1998, **13**, (1), pp. 73–77
- [41] Qian, W., Wang, L., Chen, M.Z.Q., *et al.*: 'Local consensus of nonlinear multiagent systems with varying delay coupling', *IEEE Trans. Syst., Man, Cybern., Syst.*, 2018, **48**, (12), pp. 2462–2469
- [42] Li, Y., He, L., Liu, F., *et al.*: 'Flexible voltage control strategy considering distributed energy storages for DC distribution network', *IEEE Trans. Smart Grid*, 2019, **10**, (1), pp. 163–172
- [43] Li, Y., Li, J., Qi, J., *et al.*: 'Robust cubature Kalman filter for dynamic state estimation of synchronous machines under unknown measurement noise statistics', *IEEE Access.*, 2019, **7**, pp. 29139–29148 DOI: 10.1109/ACCESS.2019.2900228